

# Global Quantum Efficiency Simulation with RAT

Thomas Wester

<https://github.com/tbwester/ratpac-nudot/>

(Dated: July 24, 2017)

## CONTENTS

I. Introduction	1
II. Geometry	2
A. The Bo Cryostat	2
B. Source Holder	2
C. TPB Plate & PMT	3
D. Material Parameters	3
III. Analysis & Results	4
A. Rayleigh Scattering	4
B. Reflectivity	5
C. Source to PMT Simulation	5
D. Systematic Errors	8
References	8

## I. INTRODUCTION

This note describes the optical photon simulation created to accompany measurements made with MicroBooNE PMTs in the Bo cryostat. The purpose of the measurements is to determine the global quantum efficiency (GQE) of the MicroBooNE optical units, which consist of a wavelength-shifting plate and a photomultiplier tube (PMT). A measurement for the GQE was determined by measuring an observed quantity of photoelectrons (PEs) from the PMT, combined with an estimate of the number of photons which hit the plate, corresponding to that particular PE number. The GQE, then, is:

$$\text{GQE} \equiv \langle Q \rangle = \frac{\# \text{ PE}}{\# \text{ Photons Hits on the Plate}} \quad (1)$$

Data was taken using a Polonium alpha source which is estimated to produce  $134000 \pm 400$  photons per decay in liquid argon. This source holder was placed at two distances away from the plate,  $d = 20.3\text{cm}$  and  $d = 36.8\text{cm}$ .

This simulation uses RAT, a software package based around GEANT4, to handle the ray tracing and the interactions of photons with the various materials in the cryostat. The objective of the simulation is to confirm the PE measurement made previously, and determine a value for the corresponding number of photons which hit the TPB plate at both  $d$  positions of the source.

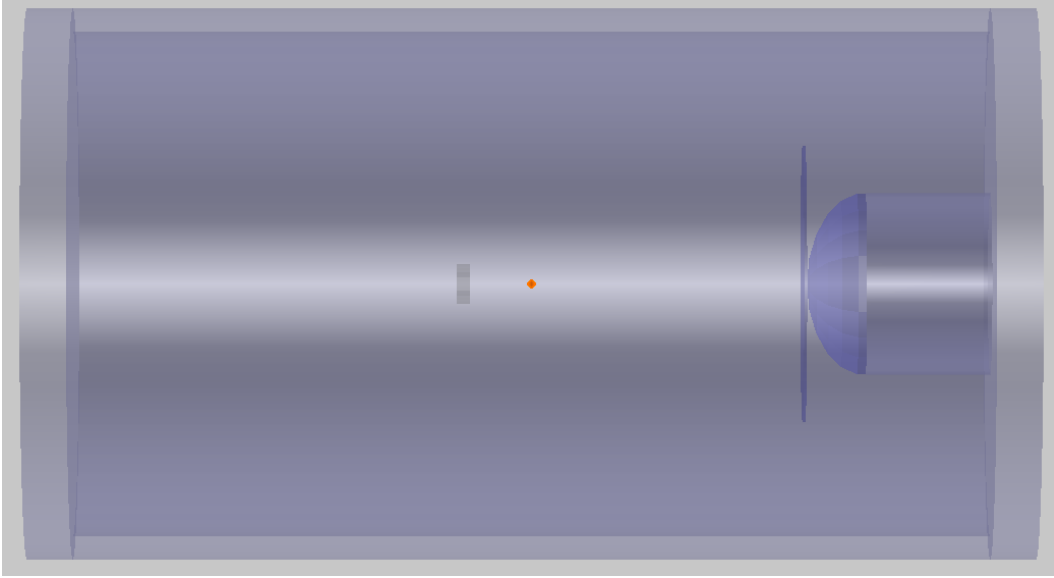


FIG. 1: A view of the simulated Bo cryostat geometry showing (from left to right) the source holder, TPB plate, PMT glass and PMT metal shield. The origin in the simulation coordinate system is the orange point.

## II. GEOMETRY

The Bo optical photon simulation uses the following convention: the positive  $z$ -direction points from the top of the cryostat towards the bottom, where the TPB plate and PMT are located. The  $x$ - $y$  plane is perpendicular and azimuthal symmetry is assumed (although the simulation is fully 3-D) for some analyses. The origin is placed at the center (depth-wise and width-wise) of the cryostat volume. Every quantity listed in inches is converted to centimeters with the factor 2.54. An overview of the geometry is shown in Figure 1.

### A. The Bo Cryostat

The Bo cryostat is a cylindrical volume 40 inches in depth and 11 inches in inner-radius. Two end caps are placed with inner faces at  $z = \pm 20$  inches to enclose the volume.

### B. Source Holder

The source holder is centered in the  $x$ - $y$  plane and is varied in position along the  $z$ -axis. The holder is modeled using two stacked ring volumes and an additional solid cylinder. A cross section is shown in Figure 2. The top two rings total in height to form the source collimator. The source itself is placed 0.01mm above the back of the collimator to simulate (i) the thickness of the aluminum foil on which the polonium is deposited and (ii) the potential for backscatters of photons reflecting on the aluminum.

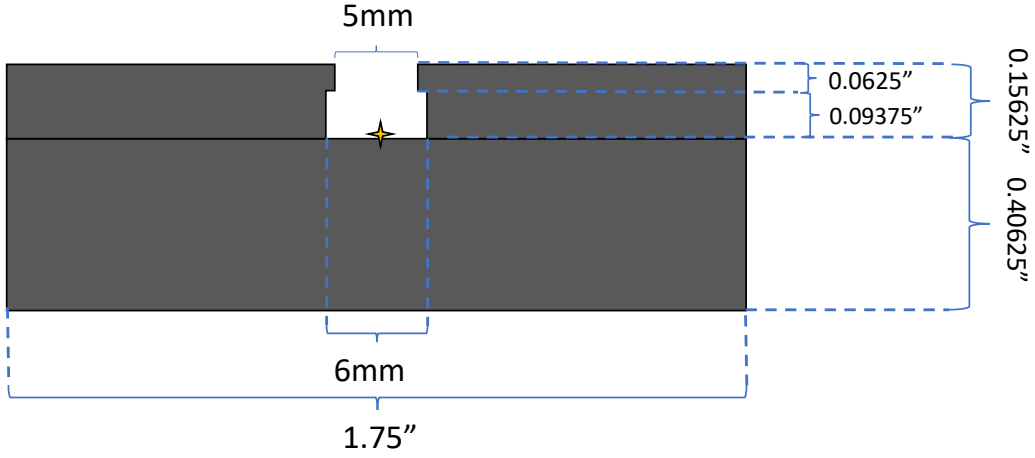


FIG. 2: To-scale cross-section of the source holder, with relevant dimensions labeled, using the primary source holder configuration. The source, a point indicated with a star, is placed just above the back of the collimator.

There are two sets of measurements for the source holder. The first set, henceforth the “primary” set, as reported by Ben Jones, has the height of the inner chamber at 0.09375 inches. The second configuration, measured by Fermilab radiation staff, has this same height at 0.1 inches. In either case, the total depth of the collimator (0.15625”) is the same. Additionally, the second set has slightly wider collimator radii, at 2.58 mm and 3.18 mm respectively. The effect of switching the geometry configuration is discussed in Section III D.

### C. TPB Plate & PMT

The TPB plate is an acrylic disk 15.24 cm. The plate is placed with its center at the origin in the  $x$ - $y$  plane and at a fixed position of  $z = 30$ cm (front face). The PMT is modeled as a hollow ellipsoid with minor axis pointing along the  $z$ -direction at 65mm in length. The major axes in the  $x$  and  $y$ -directions are identical with length at 101mm. The thickness of the ellipsoid is 0.5mm throughout. The PMT position is set according to the back face of the TPB plate, such that the closest point of the ellipsoid is 1/8 inch away from the back face of the TPB plate.

The geometry parameters for each detector component are summarized in Table I.

### D. Material Parameters

Table II lists each simulation feature, its material, and the associated index of refraction,  $N$ , and reflectivity,  $R$ . Note that  $N$  and  $R$  have different values depending on the wavelength of the incident photon.

Additionally, we assign the Rayleigh scattering length parameter in LAr as  $\lambda = 60 \pm 6$  cm [3]. The absorption length for pure liquid argon is greater than 1 km [6], and therefore

Quantity	Value	-
Cryostat Inner Radius	11"	-
Cryostat Depth	40"	-
Collimator Depth 1	0.0625"	-
Collimator Depth 2	0.09375"	-
Collimator Radius 1	2.5 mm	-
Collimator Radius 2	3mm	-
TPB Plate Radius	12"	-
TPB Plate Depth	0.125"	-
PMT Glass Thickness	0.5mm	-
PMT Glass Major Axis	101mm	-
PMT Glass Minor Axis	65mm	-

TABLE I: Summary of relevant geometry parameters and associated uncertainties (where applicable). Note that the collimator has two associated radii and depths, see Figure 2.

Feature	Material	$N$ (128/420nm)	$R$ (128/420nm)
Source Holder	Aluminum	-	$0.2 \pm 0.1$ [1] / -
Cryostat Walls	Stainless Steel	-	0.35 / $0.540 \pm 0.005$ [2]
Cryostat Interior	LAr	$1.45 \pm 0.07$ [3] / $1.23 \pm 0.002$ [4]	-
TPB Plate	Acrylic	- / $1.49 \pm 0.2$ [4]	-
PMT Window	Glass	- / $1.46 \pm 0.04$ [5]	-

TABLE II: Summary of material properties relevant to the optical simulation. Note that some values are omitted if they are negligible: light produced in the TPB plate is unlikely to reflect on the aluminum source holder. The PMT is not sensitive to 128 nm light, so  $N_{\text{Glass}}$  is not used in this simulation for that wavelength.

is not relevant to this test.

### III. ANALYSIS & RESULTS

The simulation consists of two steps to imitate the wavelength-shifting effect of the TPB plate. The first step propagates 128nm photons from the source holder to the plate, while the second step propagates 420nm photons from the plate to the PMT. The analysis consists of general physics checks, and the creation of a simulated PE spectrum by combining the two simulation steps.

#### A. Rayleigh Scattering

Rayleigh scattering has two properties relevant to the optical simulation. First, the probability of scattering is exponential with parameter  $\lambda$ . Second, the distribution of scattering angles,  $\theta_s$ , is proportional to  $1 + \cos^2 \theta_s$ .

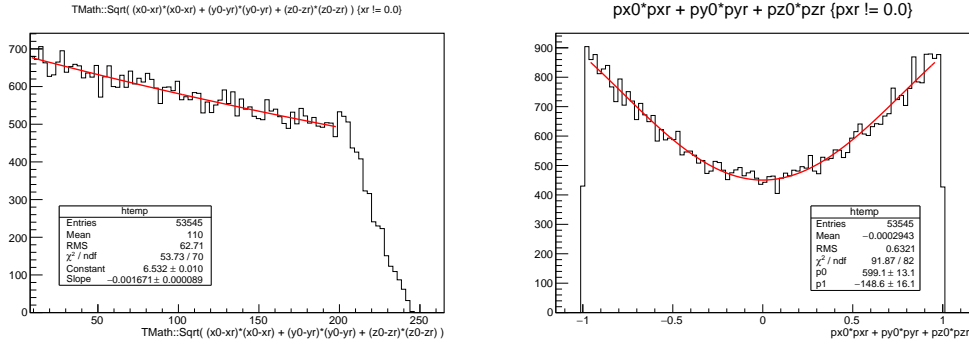


FIG. 3: Left: Exponential function fitted to the distance between photon starting points and corresponding locations of Rayleigh scattering, showing good agreement with the parameter  $\lambda = 60$  cm (Note: the fit parameters are in units of mm, and ROOT is fitting the form  $\exp[1/\lambda]$ . The drop in events at high distances is due to photons hitting the detector walls, etc.). Right: Dot product of initial photon direction with direction after Rayleigh scattering, fitted with a  $1 + \cos^2 \theta$  distribution, also showing good agreement.

Both of these properties are implemented within RAT. To test them, we save the initial position and direction of each photon as well as the position and direction at the instance of first scattering. We can then examine the distributions of the scattering lengths and scattering angle dot product, and fit these distributions to the expected functional form. This is shown in Figure 3.

## B. Reflectivity

We assign a nominal value of 0.10 for the reflectivity of aluminum [1]. We can check the initial direction of photons to see the effect of this parameter on the observed number of TPB plate hits. In Figure 4, we show the number of hits as a function of the cosine of the starting angle,  $\cos \theta_0$ , i.e. the direction the photon is pointing along the  $z$ -axis. The photon source was placed centered on the  $x$ - $y$  axis for this test. A cut selecting only those events with negative  $\cos \theta_0$ , and that did not undergo scattering, gives 12000 events, out of the total 123000 events. This is consistent with the set reflectivity value, noting the asymmetry of the collimator chamber (see Figure 2).

## C. Source to PMT Simulation

The full simulation involves the combination of weighting several steps.

1. The probability of a 420 nm photon created in the TPB plate registering as a hit on the PMT is found as a function of hit position on the plate. In RAT, a point source is placed at a fixed depth in the TPB plate, and moved along the radius of the TPB plate in steps. At each step, a number of photons is generated and tracked through to the PMT. The number of photons that register as hits on the PMT, divided by the total number of photons generated at each radial position gives the efficiency curve shown in Figure 6 (left).

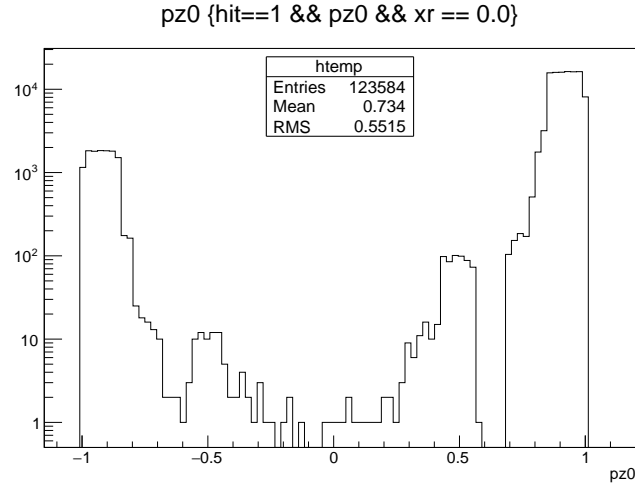


FIG. 4: Log-scale plot showing the angular distribution of photons from the source holder which hit the TPB plate.

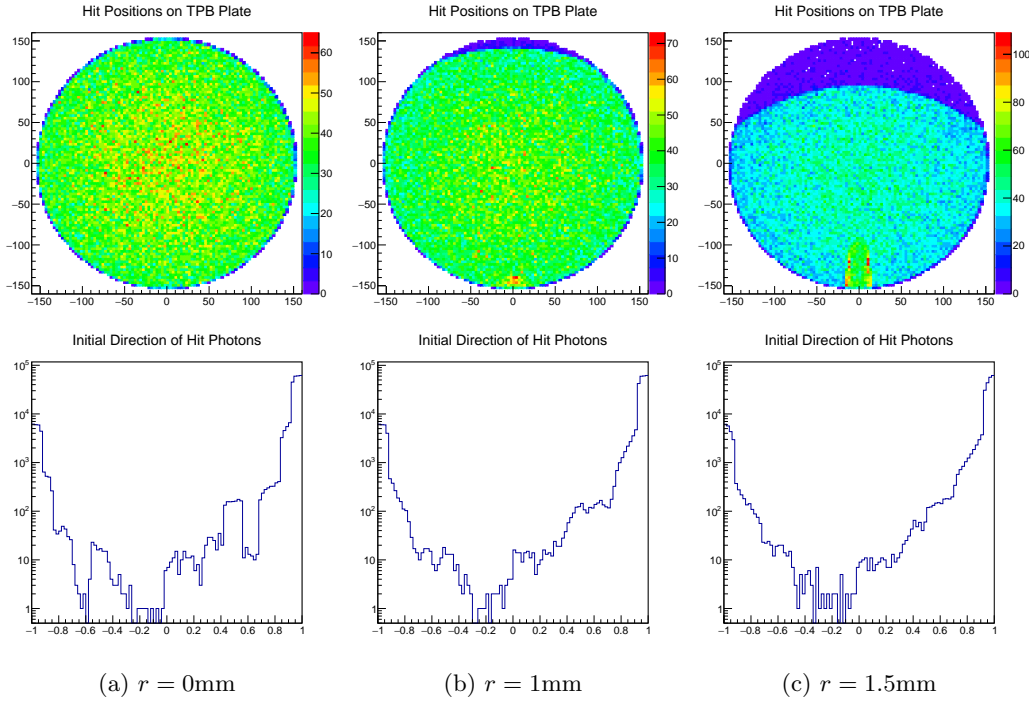


FIG. 5: Plots associated with  $d = 36.8\text{cm}$ . Top row: Hit positions on the TPB plate (units mm) as a function of the source position in the source holder,  $r$ , showing eclipsing as the source is moved behind the outer collimator cylinder. Bottom row: Initial directions ( $\cos \theta_0$ ) of hitting photons.

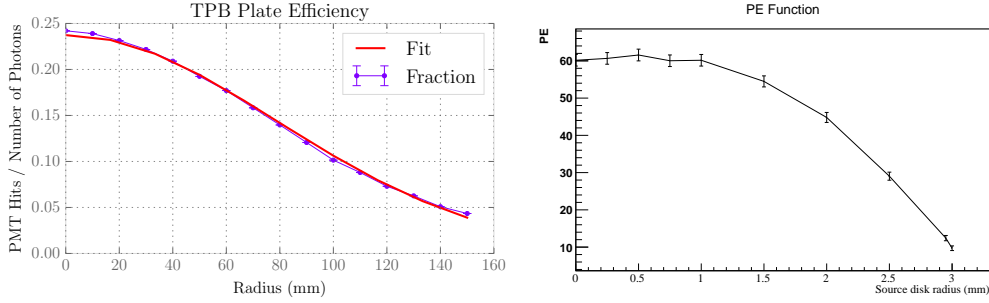


FIG. 6: Left: Percentage of 420 nm photons produced in the TPB plate which reach the PMT. The red curve is a Gaussian fit, with  $\sigma = 80$ . Right: photoelectrons as a function of source position in the source holder, for both  $d = 20.3$  and  $d = 36.8$ .

2. The distribution of hits on the TPB plate is found as a function of starting position in the source holder. Several sample distributions are shown in Figure 5. In this step, 128 nm photons are created in the aluminum source holder and propagate through the liquid argon volume. The positions of photons that hit the TPB plate are saved and convolved with (1). The convolution is done by calculating the distance from each hit position to the center of the TPB plate, and linearly interpolating along the curve shown in Figure 6 (left) to compute a “weighted hit”. The weighted hits are summed to give the mean number of photons registered on the PMT at each source position. This is shown in Figure 6 (right), in units of photoelectrons. The multiplicative factors used to convert weighted hits into PE are:

- $1.18 \pm 0.1$  efficiency of 128 nm light re-emitting 420 nm light in the TPB plate, coated via evaporation.
- 0.64 relative efficiency of the plate to our own plate, which is dipped in TPB instead of coated via evaporation.
- 0.199 quantum efficiency of the MicroBooNE PMTs

Finally, we expect  $134000 \pm 6000$  photons per alpha decay. We scale the final number of PEs by the ratio of this number to the number of simulated photons.

3. To generate an expected photoelectron spectrum, we convolve the curves shown in Figure 6 (right) with a simple Monte Carlo. Points are randomly selected within the area of the source disk following a bivariate normal distribution with  $x$  and  $y$  positions independent, and  $\sigma =$ . The distance from each point to the source disk origin is calculated, and the corresponding photoelectrons at that distance are computed by linearly interpolating along the curves from Figure 6 (right). The last step is to simulate a Poisson process governing the PE distributions. The results of this step are shown in Figure 7.

The final PE spectrum from (1)-(2)-(3) above can be fitted to obtain the expected number of observed PE for a given distance. The results of running the full simulation, and fitting the final PE spectrum, using the nominal simulation parameters are presented in Table III. The final list of all parameter nominal values and uncertainties is outlined in Table IV.

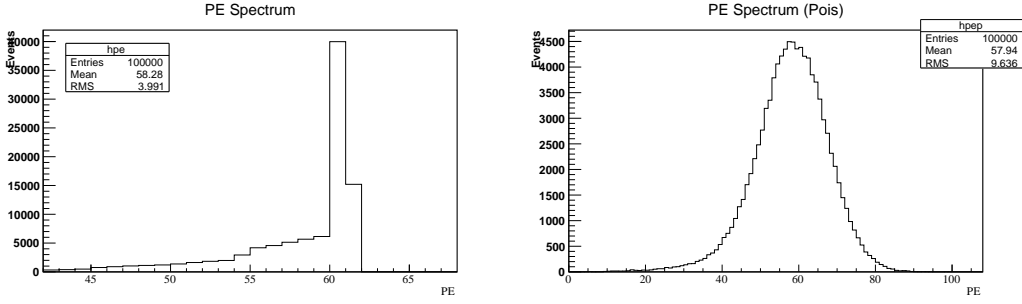


FIG. 7: Left: Distribution of PE from source emission Monte Carlo. Left: Poisson-smeared distribution, showing the observed PE peak.

$d$ (cm)	PE	Plate Hits	$\langle Q \rangle$
20.3	166.6		
36.8	58.8		

TABLE III: Summary of simulation results, using the nominal values summarized in IV. Note that the number of plate hits is scaled based on the simulation size, so that PE and plate hits can be compared to experimental values.  $\langle Q \rangle$  is the ratio, via Equation 1.

#### D. Systematic Errors

The RAT simulation is sensitive to some parameters and insensitive to others. Following the analysis steps outlined previously, the full RAT simulation is run several times, varying each parameter by its estimated  $1\text{-}\sigma$  value. The change in the number of PE due to changing each parameter by its  $1\text{-}\sigma$  value is summarized in Table IV. Note that absolute values are taken, and that these tests were done by testing the upper limits only.

- 
- [1] M. C. Johnson, *Applied Optics* **7**, 879 (1968).
  - [2] E. W. Spisz, A. J. Weigund, R. Bowmun, and J. R. Jack, *NASA Technical Note* **5353** (1969).
  - [3] E. Grace, A. Butcher, J. Monroe, and J. A. Nikkel, *Nuclear Instruments and Methods in Physics Research Section A: Accelerators, Spectrometers, Detectors and Associated Equipment* **867**, 204208 (2017).
  - [4] A. C. Sinnock and B. L. Smith, *Physical Review* **181**, 12971307 (1969).
  - [5] I. H. Malitson, *Journal of the Optical Society of America* **55**, 1205 (1965).
  - [6] B. J. P. Jones, C. S. Chiu, J. M. Conrad, C. M. Ignarra, T. Katori, and M. Touns, *Journal of Instrumentation* **8** (2013), 10.1088/1748-0221/8/09/e09001.



Parameter	Value	1- $\sigma$	PE, $d = 20.3$	PE, $d = 36.8$	% Change
Source Distribution Width	0.08mm	$\pm 0.07$ mm	155.3		6.8
Source Height in Holder	0.01cm	$\pm 0.002$ cm	165.8	58.7	0.33
$N_{\text{LAR}}, 128 \text{ nm}$	1.45	$\pm 0.07$		61.8	5.1
$N_{\text{LAR}}, 420 \text{ nm}$	1.23	$\pm 0.002$		58.8	0
$N_{\text{Acrylic}}, 420 \text{ nm}$	1.49	$\pm 0.02$	153.2		8.04
$N_{\text{Glass}}, 420 \text{ nm}$	1.46	$\pm 0.04$		57.8	1.7
$R_{\text{Al}}, 128 \text{ nm}$	0.1	+0.2	234.1		41
$R_{\text{Al}}, \text{Type}$	Specular	Diffuse		59.3	0.85
$R_{\text{Stainless}}, 128 \text{ nm}$	0.35				
$R_{\text{Stainless}}, 420 \text{ nm}$	0.540	$\pm 0.005$	167.5		0.54
$R_{\text{Stainless}}, \text{Type}$	Specular	Diffuse		59.4	1.02
$d$	20.3/36.8cm	4mm			
Collimator Width 1	2.5mm	+0.07*	169.1	59.1	1.01
Collimator Width 2	3.0mm	+0.18*	-	-	
Collimator Height	0.15625in	-0.025in			
Plate to PMT Distance	0.125in	$\pm 0.03$ in	159.7		4.1
Glass Thickness	0.5cm			59.0	0.34
Evap. TPB Efficiency	1.18	$\pm 0.1$			8.5
Rel. Efficiency to Evap. TPB	0.64				
PMT Quantum Efficiency	0.199				
$N_\gamma$ , Alpha	134000	$\pm 6000$			4.4
<b>Quadrature Sum</b>	-	-	-	-	15.9
<b>Nominal Sim. Values</b>	-	-	166.6	58.8	-
<b>Data</b>	-	-	74.1	28.5	-

TABLE IV: Summary of systematic uncertainty sources in the RAT simulation, as they relate to the nominal PE value. The parameters are grouped by source positioning, material parameters, geometry parameters, and multiplicative factors. PE values computed with each parameter set to the +1- $\sigma$  value.

\*Vary together.